Journal of Crystal Growth 468 (2017) 399–402

Contents lists available at ScienceDirect

Journal of Crystal Growth

journal homepage: www.elsevier.com/locate/jcrysgro

Effects of Na co-doping on optical and scintillation properties of Eu:$LiCaAlF_6$ scintillator single crystals

Chieko Tanaka[a,*], Yuui Yokota[b], Shunsuke Kurosawa[b], Akihiro Yamaji[a], Yuji Ohashi[a], Kei Kamada[b,c], Martin Nikl[d], Akira Yoshikawa[a,b,c]

[a] Institute for Materials Research, Tohoku University, Sendai, Japan
[b] New Industry Creation Hatchery Center (NICHe), Tohoku University, Sendai, Japan
[c] C&A corporation, Sendai, Japan
[d] Institute of Physics AS CR, Prague, Czech Republic

ARTICLE INFO

Communicated by Prof. S. Uda

Keywords:
A1. Doping
A2. Single crystal growth
B1. Lithium compounds
B2. Scintillator materials

ABSTRACT

Na co-doped Eu: $LiCaAlF_6$ (Eu, Na: LiCAF) single crystals were grown by the micro-pulling-down (μ-PD) method, and their optical and scintillation properties were examined to reveal the effects of the Na co-doping. The crystals were single-phase materials demonstrating structure isomorphic with that of undoped LiCAF. To perform the crystals characterization, the specimens with dimensions of several millimeters were cut from highly transparent and crack free fragments of the crystals and polished. It was observed that Na co-doping resulted modification of the transmittance and the excitation spectra, and increased the light yield detected under neutron irradiation.

1. Introduction

The neutron detectors operated using neutron scintillators have been developed for number of applications mostly utilized by the homeland security services. It is expected that demand for such devices will continue to grow because of shortage of the ^{3}He gas proportional counters following from the ^{3}He gas supply crisis [1]. In the past, we have developed the Ce- and Eu-doped $LiCaAlF_6$ (Ce:LiCAF and Eu:LiCAF) neutron scintillating single crystals with a large capture cross-section to thermal neutrons by using ^{6}Li enrichment [2–5]. The effective atomic number and the density of the LiCAF are relatively low, and this is considered as advantageous property regarding low sensitivity of the materials to γ-rays. The large bulk single crystals of Ce:LiCAF and Eu:LiCAF can be grown by the general melt growth methods and these crystals are not hygroscopic.

The Eu:LiCAF scintillating crystal demonstrates high light yield when exposed to thermal neutron irradiation while it has somewhat longer decay time [6,7]. In addition, the light yield of the Eu:LiCAF crystal was improved by its co-doping with the alkali metals (Na^+, K^+, and Rb^+ ions) [8]. However, the detailed mechanism of the light yield improvement as a result of the alkali metal co-doping was not clearly understood. Moreover, the dependence of the light yield on the content of co-dopant(s) was not reported. Therefore, this project was initiated to grow number of Na co-doped Eu:LiCAF (Eu, Na:LiCAF) single crystals with various Na concentrations, and to perform measurements of their optical and scintillation properties. The goal of this study was to reveal the mechanism of the Na co-doping effects, and influence of the Na concentration on optical and scintillation properties of the crystals.

2. Experimental procedure

The Eu:LiCAF and Eu, Na:LiCAF single crystals were grown by the micro-pulling-down (μ-PD) method in a vacuum tight chamber [9]. Starting materials, LiF (^{6}Li 95%, 4N), CaF_2, AlF_3, EuF_3, and NaF (4N purity) powders, were mixed at nominal compositions of $Li(Ca_{0.98-x}Eu_{0.02}Na_x)AlF_6$ (x=0, 0.0001, 0.0005, 0.001). To perform the growth process, the powders were charged into a carbon crucible with a ϕ2 mm outlet at the bottom. Thereafter, the crucible and a carbon insulator were placed at the center of a high-frequency induction coil in the chamber. Then, the interior of the chamber was evacuated up to ~10^{-4} Pa pressure, and the crucible was heated to ~300 °C to remove oxygen and moisture contaminations remaining on the surfaces of the starting materials, the crucible, the insulator, and other parts of the equipment. After the baking process, the chamber was filled with high purity Ar/CF_4 mixed gas (Ar: CF_4 =9: 1) up to the ambient pressure. Finally, the crucible was heated up to the melting point of the LiCAF (~814 °C) to produce the melt ready for the crystal growth. The growths were performed at 0.1 mm/min pulling-down rate using a platinum wire as a seed to initiate solidification of the melt. The grown

* Corresponding author.

http://dx.doi.org/10.1016/j.jcrysgro.2016.11.012

Available online 09 November 2016

crystals were cut and polished to produce the specimens acceptable for the measurements of their luminescent and scintillation properties. Dimensions of the polished specimens were (5–7) ×2×1 mm^3 and the thickness was 1 mm in the measurements of the optical and scintillation properties. All the specimens were produced from the transparent and crack-free parts of the crystals positioned at the distance of 5–10 mm from the seeding points. These specimens were then used for evaluation of the luminescent and scintillation properties of the crystals with almost same Eu concentration.

Transmittance spectra of the grown crystals were measured by a spectrophotometer (JASCO V-550) in the wavelength range from 190 to 800 nm. Chemical compositions were measured by the electron probe micro-analyzer [EPMA] (JEOL JXA-8530F). Powder X-ray diffraction (XRD) measurements were performed to identify the phases presenting in the grown crystals (Brucker, D8 Discover). The X-ray rocking curve (XRC) measurements of the polished specimens were performed using RIGAKU ATX-E with a 4-bounce Ge (220) channel-cut monochromator. The ω scan profiles on the (114) diffraction peak were obtained and the full width at half maximum (FWHM) of the XRC was estimated from the observed profiles. Photoluminescence spectra (PL) (emission and excitation spectra) of the polished specimens were measured by the spectrofluorometer (EDINBURGH INSTRUMENTS FLS920). The pulse-height spectra and decay curves of the polished crystals were recorded under neutron irradiation produced by the ^{252}Cf source. The measurements were performed with a photomultiplier tube (PMT) (Hamamatsu R7600U-200) and set into lead blocks to estimate the light yield and decay time. A paraffin block was used as the moderation to the neutron from the ^{252}Cf source. The specimens were covered with a Teflon tape except one face which was attached to the light entrance window of the PMT with optical grease. A Li-Glass (8,000 photons/neutron) was used as a reference. The scintillation decay curves of the specimens were measured by the oscilloscope (Tektronix TDS3052B).

3. Results and discussions

General appearance of the Eu, Na:LiCAF single crystals grown by the μ-PD method is illustrated in Fig. 1. All the as-grown crystals were approximately 2 mm in diameter and they were colorless and transparent. Some cracks were observed at the initial parts of the grown crystals due to the platinum wire seed. However, the middle parts of the crystals didn't include any cracks. Polished specimens with 1 mm thickness were prepared from the clear parts of the crystals without visible cracks. Surfaces of all specimens were polished carefully under same condition and the surface conditions are considered to be same in the all specimens.

According to the results of the EPMA, actual Eu concentrations were 0.45~0.60 mol% in specimens. They were smaller than the nominal compositions due to the small segregation coefficient of the Eu ion in the LiCAF single crystal. The small difference of the actual Eu concentration among specimens has little effect on the scintillation

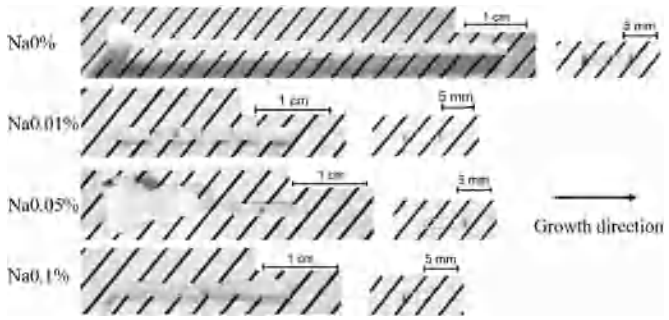

Fig. 1. View of the as grown Eu:LiCAF and Eu, Na:LiCAF crystals (left) and corresponding polished specimens (right).

properties. Unfortunately, Na couldn't be detected by the EPMA because the actual Na concentration in the specimens were lower than the detection limit of the EPMA.

Powder XRD measurements of the ground Eu, Na:LiCAF crystals were performed to identify the phases present in the as produced solids and to calculate their lattice parameters (Fig. 2(a)). All the diffraction peaks of all the grown crystals were identified as those corresponding to the LiCAF structure and no diffraction peaks representing any secondary phase were distinguished except for the diffraction peak of the EuF_3 phase formed in the Eu2%:LiCAF crystal (x=0). No peak shifts as a result of Na co-doping were detected on the diffraction patterns. The lattice parameters of Eu2%Na0.01%:LiCAF were a=5.008 Å, c=9.643 Å and it was same as Eu2%:LiCAF. Thus, it suggests that the actual concentrations of the Na ion in the crystals is too low to have an effect on the lattice parameters of the LiCAF structure.

The XRC measurements of the polished specimens were performed to examine the effect of the Na co-doping on the crystallinity of the Eu:LiCAF crystals (Fig. 2(b)). The Na0.01% and 0.05% co-doped specimens demonstrated a sharp single peak in the XRC while there were some satellite peaks in addition to a sharp peak in the XRC of the non-codoped and Na0.1% co-doped specimens. The satellite peaks are considered to be due to the EuF_3 impurity which was observed in the XRD pattern or subgrains in the crystals. The FWHM's of the XRC's for Eu2%:LiCAF and Eu2%Na0.01, 0.05, 0.1%:LiCAF were 173 (0.048°) and 39.6 (0.011°), 20.88 (0.0058°) and 180.0 arcsec (0.050°), respectively. These results confirmed that there was no degradation of the crystallinity associated with the Na co-doping up to 0.05%.

The transmittance spectra of the polished Eu:LiCAF and Eu, Na:LiCAF specimens were measured and the results are illustrated in Fig. 3(a). All the specimens had greater than 70% transmittance in the wavelength range from 380 to 800 nm. Absorption peaks around 200 and 300 nm were observed for all the crystals and they were attributable to the 4f-5d transitions of the Eu^{2+} ion [6,7]. On the other hand, the positions of the edges of the absorption peaks around 350 nm and the transmittance around 320 nm were different that was result of various levels of Na co-doping. Fig. 3(b) shows the PL spectra of the polished Eu:LiCAF and Na, Eu:LiCAF specimens. In the emission spectra recorded under 340 nm excitation, an emission peak was observed around 370 nm and the wavelength was almost consistent with the previous report [7]. No peak shift associated with different level of Na co-doping was detected on the emission spectra. Meanwhile, the excitation spectra around 350 nm were changed depending on Na co-doping and Na concentration. The reason of the changes in the transmittance and excitation spectra with Na co-doping are not clear and need further study.

Pulse-height spectra and decay curves of the Eu:LiCAF and Eu, Na:LiCAF polished specimens observed under neutron irradiation were also measured, and the results are illustrated in Fig. 4. All the specimens demonstrated a peak in the pulse-height spectra and the light yields were estimated by comparing the newly obtained results with those available for the Li-Glass (Fig. 4(a)). The estimated light yields of the Eu2%:LiCAF and the Eu2%Na 0.01%, 0.05% and 0.1%:LiCAF specimens were 21,800, 24,500, 21,000, and 19,800 photons/neutron, respectively and the Eu2%Na0.01%:LiCAF had the maximum light yield. However, the light yields of all these specimens were lower than that in the previous report and the suitable Na co-dopant concentration was also different from that reported in the past [5]. The differences of the light yield and the suitable Na co-dopant concentration are suggested to be attributable to the difference of the actual Eu concentration in the specimens. In this study, we evaluated the specimens cut from the fragments positioned relatively close to the initial parts of the crystals neighboring the seed. Therefore, the actual Eu concentration in the crystals were relatively low when compared to their nominal composition as referred above. As a result, low actual Eu concentration in LiCAF resulted lower light yield and the lower suitable concentration of Na co-dopant.

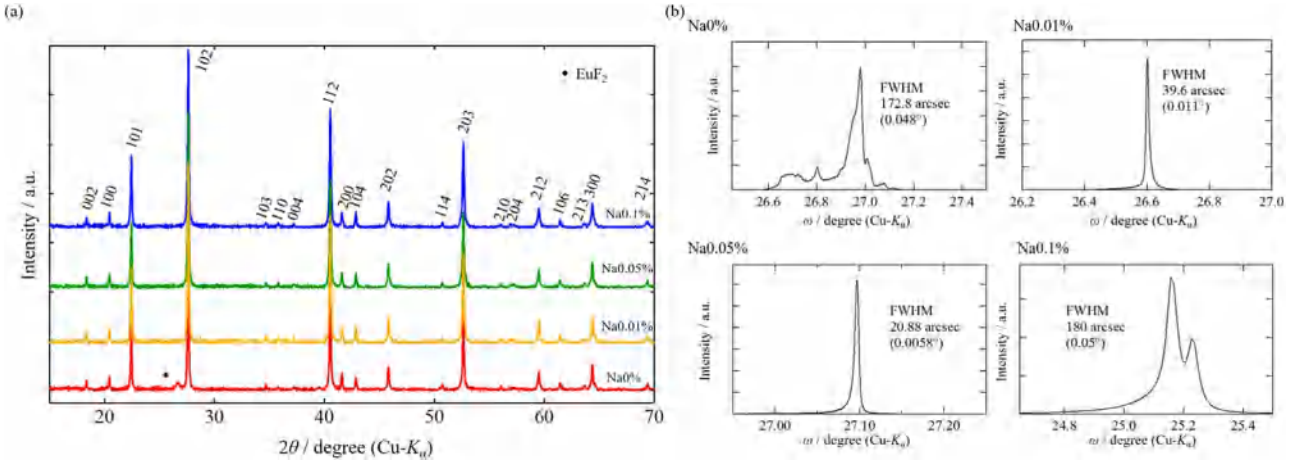

Fig. 2. (a) Powder XRD patterns and (b) XRC's of the Eu:LiCAF and Eu, Na:LiCAF crystals.

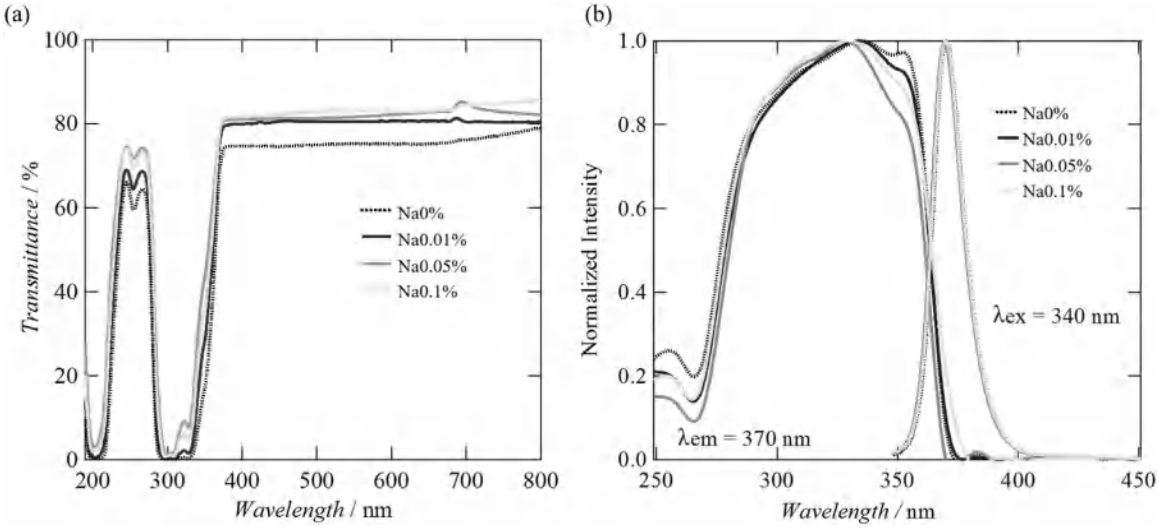

Fig. 3. (a) Transmittance (a) and PL spectra of the Eu: LiCAF and Na, Eu: LiCAF polished specimens.

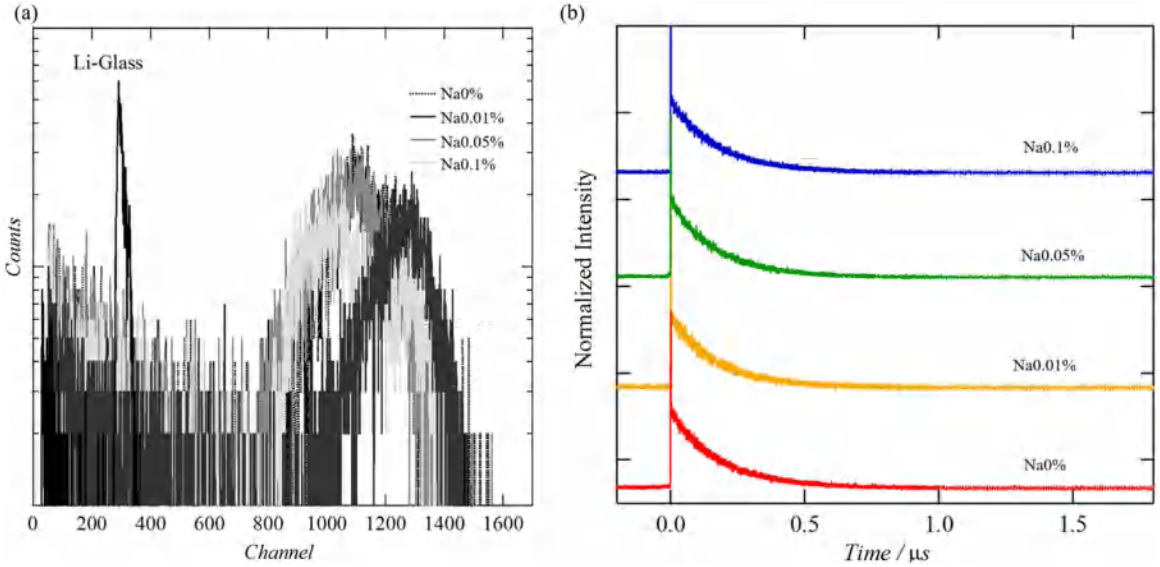

Fig. 4. (a) Pulse-height spectra and (b) decay curves of the Eu: LiCAF and Na, Eu: LiCAF polished specimens observed under thermal neutron irradiation.

The decay curves of the specimens are shown in Fig. 4(b). The decay times were estimated by fitting the curves using the single exponential decay function. The estimated decay times of the Eu:LiCAF and the Na 0.01%, 0.05% and 0.1%, Eu:LiCAF specimens were 1.81, 1.69, 1.69 and 1.72 μs, respectively. The variation of the decay time is not so large and it doesn't have a significant physical meaning.

There are two possible mechanisms of the Na co-doping effects on the luminescence and scintillation properties according to the previous reports about the Ce doped garnet scintillator with co-dopant [10,11]. In the Ref. [10], the Ce^{4+} ion is generated by the Mg^{2+} co-doping to the Ce^{3+}:$Lu_3Al_5O_{12}$ single crystal and the stable Ce^{4+} center provides an additional fast radiative recombination pathway in the scintillation mechanism and efficiently competes with electron traps. In the result, the light yield was increased by the Mg^{2+} co-doping. On the other hand, in the Ref [11] Mg^{2+} co-doping to the Ce^{3+}:$Gd_3Al_2Ga_3O_{12}$ single crystal works to obstruct the formation of shallow electron traps and the Mg^{2+} co-doping improved the scintillation properties. Therefore, in the Na^{+} doped Eu^{2+}:LiCAF single crystal, the following possible mechanisms can be considered: (1) Eu^{3+} were formed by the Na co-doping and the Eu^{3+} center contribute to the luminescence. (2) Na^{+} co-dopant works to obstruct the formation of shallow electron traps in Eu:LiCAF single crystals and this causes the improvement of the scintillation properties. In this study, we confirmed the Na co-doping effects on the luminescence and scintillation properties in Eu:LiCAF. However, we need further studies to reveal the detailed mechanism of Na co-doping.

4. Conclusions

Na co-doped Eu:$LiCaAlF_6$ single crystals with various Na concentrations were grown by the μ-PD method, and their phase purity, crystallinity, optical and scintillation properties were examined. While there was no wavelength shift of the emission peak in the PL spectra followed the Na co-doping, transmittance and excitation spectra were locally changed around 320 and 350 nm. In addition, the Na0.01% co-doping increased the light yield by 10% by the Na co-doping as well. Thus 0.01% Na concentration seems the optimum one to improve scintillation characteristics. However, the Na0.1%, Eu:LiCAF crystal demonstrated the light yield lower than that of Eu:LiCAF.

Acknowledgements

This work is partially supported by the New Energy and Industrial Technology Development Organization (NEDO), the Japan Society for the Promotion of Science (JSPS) Research Fellowships for Grant-in-Aid for Young Scientists, Japan Science and Technology Agency (JST) Adaptable & Seamless Technology Transfer Program through Target-driven R & D (A-STEP). Partial support of Czech project supporting Czech-Japan collaboration, MEYS KONTAKT II, no. LH14266, is also gratefully acknowledged.

References

[1] R.C. Runkle, A. Bernstein, P.E. Vanier, J. Appl. Phys. 108 (2010) 111101.
[2] A. Yoshikawa, T. Yanagida, Y. Tokota, N. Kawaguchi, S. Ishizu, K. Fukuda, T. Suyama, K.J. Kim, J. Pejchal, M. Nikl, K. Watanabe, M. Miyake, M. Baba, K. Kamada, IEEE Trans. Nucl. Sci. 56 (2009) 3796–3799.
[3] T. Yanagida, A. Yoshikawa, Y. Yokota, S. Maeo, N. Kawaguchi, S. Ishizu, K. Fukuda, T. Suyama, Opt. Mater. 32 (2009) 311–314.
[4] Y. Yokota, Y. Fujimoto, T. Yanagida, H. Takahashi, M. Yonetani, K. Hayashi, I. Park, N. Kawaguchi, K. Fukuda, A. Yamaji, Y. Fukazawa, M. Nikl, A. Yoshikawa, Cryst. Growth Des. 11 (2011) 4775–4779.
[5] T. Yanagida, A. Yamaji, N. Kawaguchi, Y. Fujimoto, K. Fukuda, S. Kurosawa, A. Yamazaki, K. Watanabe, Y. Futami, Y. Yokota, A. Uritani, T. Iguchi, A. Yoshikawa, M. Nikl, Appl. Phys. Express 4 (2011) 106401.
[6] M. Nikl, P. Bruza, D. Panek, M. Vrbova, E. Mihokova, J.A. Mares, A. Beitlerova, N. Kawaguchi, K. Fukuda, A. Yoshikawa, Appl. Phys. Lett. 102 (2013) 161907.
[7] T. Yanagida, N. Kawaguchi, Y. Fujimoto, K. Fukuda, Y. Yokota, A. Yamazaki, K. Watanabe, J. Pejchal, A. Uritani, T. Iguchi, A. Yoshikawa, Opt. Mater. 33 (2011) 1243–1247.
[8] A. Yamaji, T. Yanagida, N. Kawaguchi, Y. Yokota, Y. Fujimoto, S. Kurosawa, J. Pejchal, K. Watanabe, A. Yamazaki, A. Yoshikawa, Radiat. Meas. 55 (2013) 132–135.
[9] A. Yoshikawa, T. Satonaga, K. Kamada, H. Sato, M. Nikl, N. Solovieva, T. Fukuda, J. Cryst. Growth 270 (2004) 427–432.
[10] M. Nikl, K. Kamada, V. Babin, J. Pejchal, K. Pilarova, E. Mihokova, A. Beitlerova, K. Bartosiewicz, S. Kurosawa, A. Yoshikawa, Cryst. Growth Des. 14 (2014) 4827–4833.
[11] M. Kitaura, K. Kamada, S. Kurosawa, J. Azuma, A. Ohnishi, A. Yamaji, K. Hara, Appl. Phys. Express 9 (2016) 072602.